*34th EPS Conference on Plasma Phys. Warsaw, 2 - 6 July 2007 ECA Vol.**31F**, P-1.094 (2007)*

Statistical properties of L-mode edge plasma turbulence for three different magnetic configurations in the Mega Amp Spherical Tokamak

B. Hnat[1], B. D. Dudson[2], R. O. Dendy[3,1], G. F. Counsell[3], A. Kirk[3] and the MAST team[3]

[1]*Centre for Fusion, Space and Astrophysics, Department of Physics, Warwick University, Coventry CV4 7AL, U.K.*

[2]*Physics Department, University of York, YO10 5DD, U.K.*

[3] *Euratom/UKAEA Fusion Association, Culham Science Centre, Abingdon, Oxfordshire OX14 3DB, U.K.*

Introduction. The links between edge turbulence, energy confinement, and outer magnetic field geometry in tokamaks are highly topical [1, 2]. Quantitative characterisation of the strongly nonlinear signals obtained from probe measurements of the ion saturation current I_{sat} in tokamak edge plasmas, in relation to magnetic geometry, is thus important. It assists understanding of confinement physics and helps identify statistical properties of edge turbulence that are universal and invariant [3, 4, 5]. Here we build on a study[5] that applied modern techniques of nonlinear time series analysis [6] to three L- and H-mode plasmas in the Mega Amp Spherical Tokamak (MAST) [7], identifying a dual scaling regime. We focus on three MAST L-mode plasmas that differ in their magnetic field configurations: upper disconnected double null (UDDN), lower disconnected double null (LDDN) and connected double null (CDN); see Fig. 1. All have plasma current $I_p \approx 710$kA and line averaged electron number density $n \approx 2.4 \times 10^{19}\mathrm{m}^{-3}$.

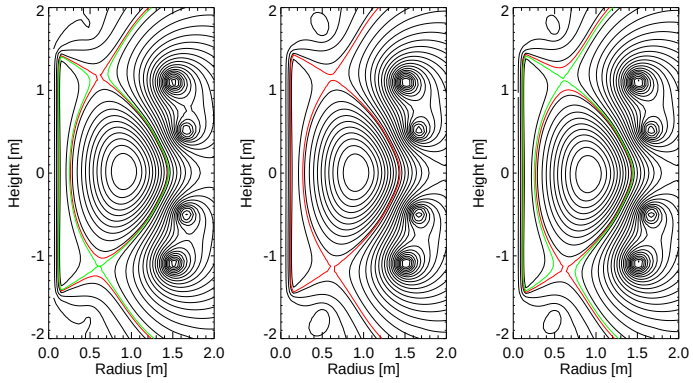

Figure 1: Poloidal projections of different magnetic field structure for three MAST plasmas examined here; (left) UDDN 14218; (centre) CDN 14219; (right) LDDN 14220. The colours are red for the inner separatrix (boundary between closed and open field-lines) and green for the outer separatrix (boundary between those field-lines open to one divertor and those open to both divertors). In the case of 14219 (CDN) only the red is shown since the two surfaces coincide to within a gyroradius at the outboard midplane.

Data and Methods. The I_{sat} datasets were obtained with a reciprocating Langmuir probe, sampling at rates of 500kHz, during periods when the distance from the probe to the plasma

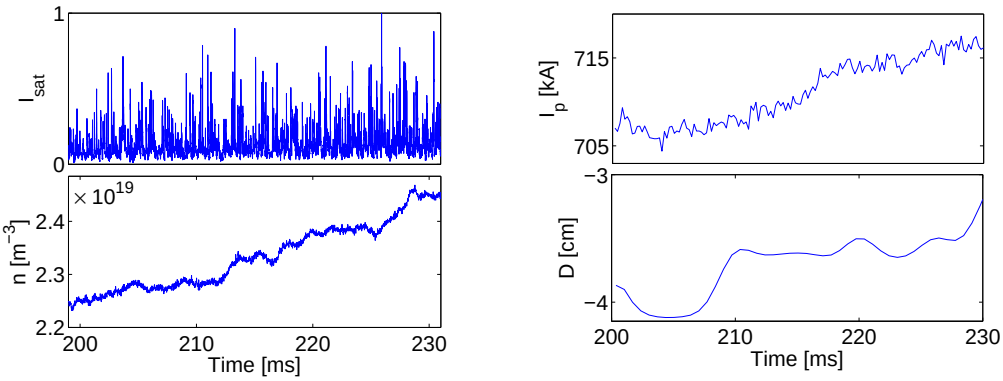

Figure 2: Examples of measurements for MAST plasma 14219: (a) detrended ion saturation current I_{sat}; (b) line averaged electron density; (c) plasma current; (d) distance from the probe to the plasma edge.

edge $D = 3.7 \pm 0.5$cm was approximately constant and the same in all cases. Figure 2 shows measured signals for the selected time interval of MAST plasma 14219. We consider normalised ion saturation signals as stochastic increments given on the temporal scale $\tau_{min} = 2\mu$s, defined by the sampling time interval between consecutive measurements. Fluctuations on longer temporal scales are obtained by summing the original signal across a window of width τ [5], $\delta I_{sat}(t,\tau) = \sum_{t'=t}^{t+\tau-\tau_{min}} (I_{sat}(t') - < I_{sat} >_t)/\sigma$, where $< ... >_t$ indicates the average over all times and σ stands for the standard deviation of the I_{sat} signal. Structure functions S_m of these fluctuations are then defined as $S_m(\delta I_{sat}, \tau) = \langle |\delta I_{sat}(t,\tau)|^m \rangle_t \propto \tau^{\zeta(m)}$ and the last proportionality on the r.h.s is valid only if S_m exhibits scaling with respect to τ for a wide range of temporal scales τ. In this case a log-log plot of S_m versus τ yields a straight line for each m and the gradient of this line gives the value of $\zeta(m)$. Generally $\zeta(m)$ can be a nonlinear function of order m, where the nonlinearity reflects intermittency. However, if $\zeta(m) = \alpha m$ (α constant) then the time series is self-affine with a single scaling exponent α. In a region where an approximate self-similarity of the fluctuations can be established, it is possible to factorise the PDF according to the formula $P(\delta I_{sat}, \tau) = \tau^{-\alpha} P_s(\delta I_{sat} \tau^{-\alpha})$, where α is a scaling exponent derived, for example, from the structure function analysis. Function $P_s(\delta I_{sat} \tau^{-\alpha})$, which does not depend on the temporal scale explicitly, defines a universal curve upon which all other PDFs will collapse when factorised. The functional form of P_s yields information on the underlying physics of the turbulence that is measured. We shall show that for each MAST plasma considered, there are two regions of scaling and that we can concentrate on the PDFs for the minimum values of τ for each region, namely $\tau = 2\mu$s and $\tau = 64\mu$s.

Results. Figures 3(a,b,c) show four absolute moments, $1 \leq m \leq 4$, as functions of the temporal scale τ for the three discharges studied here. These moments exhibit two well defined and

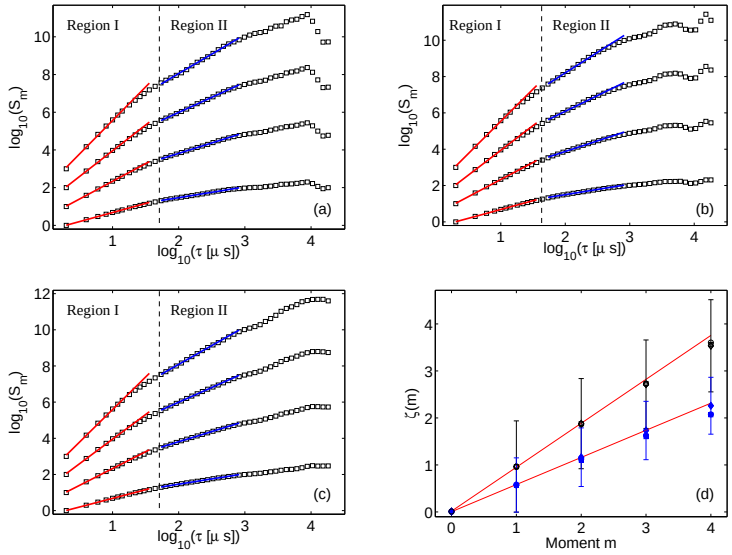

Figure 3: Moments $m=1$ (bottom traces) to $m=4$ (top traces) of the $\delta I_{sat}(t,\tau)$ fluctuations plotted versus temporal scale τ for the three MAST plasmas: (a) 14218(UDDN); (b) 14219(CDN); (c) 14220(LDDN). The curves at each order m have been offset vertically for clarity, such that $S_m^{plot} = S_m^{actual}(\tau) - S_m^{actual}(\tau = 2\mu s) + (m-1)$. (d) Scaling exponents $\zeta(m)$ plotted versus order m for MAST plasmas: $\square -$ 14218, $\diamond -$ 14219 and $\circ -$ 14220. The two solid lines represent the best linear fit $\zeta(m) = \alpha m$ with $\alpha = 0.94 \pm 0.07$ for Region I and $\alpha = 0.56 \pm 0.08$ for Region II. Error bars relate to MAST plasma 14218 and are inferred from the regression errors of the linear fits for each region.

distinct regions of scaling which may correspond to filamentary structures observed in optical imaging[8]: Region I with a slope -0.94 extending from $\tau \approx 2\mu$s to $\tau \approx 40\mu$s and Region II with a shallower slope for time scales $\tau \approx 40\mu$s to $\tau \approx 400\mu$s. The transition time is comparable to the decorrelation time estimated from the first zero crossing of the autocorrelation function[5]. Figure 3(d) presents these exponents for moments with order m ranging up to $m = 4$. We observe a clear separation of scaling exponents derived from Region I and II into two distinct groups regardless of the detailed magnetic configuration of the discharge. In all cases, the scaling exponents can be approximated by the linear relation $\zeta(m) = \alpha m$ with a constant parameter α and a constraint $\zeta(0) = 0$. The value of α is the same for all the L-mode plasmas and for both scaling regions, suggesting universality in the character of these fluctuations.

We now consider continuous models for the $\delta I_{sat}(t,\tau)$ distributions on different temporal scales derived from extreme value statistics, specifically Fréchet and Gumbel distributions. The Gumbel distribution is defined as $P_G(x,a) = C_G \exp[-a(x+e^{-x})]$, while the Fréchet distribution is given by $P_F(x,k) = C_F \exp(-x^{-k})/(x^{1+k})$, where a and k are fitting parameters. Figure 4 shows a single PDF on temporal scale $\tau = 2\mu$s(left) and $\tau = 64\mu$s(right) constructed from all three MAST plasma datasets, each normalised to its respective standard deviation. The distribution is asymmetric heavy tailed. Dashed and thick lines represent a log-normal and the Fréchet

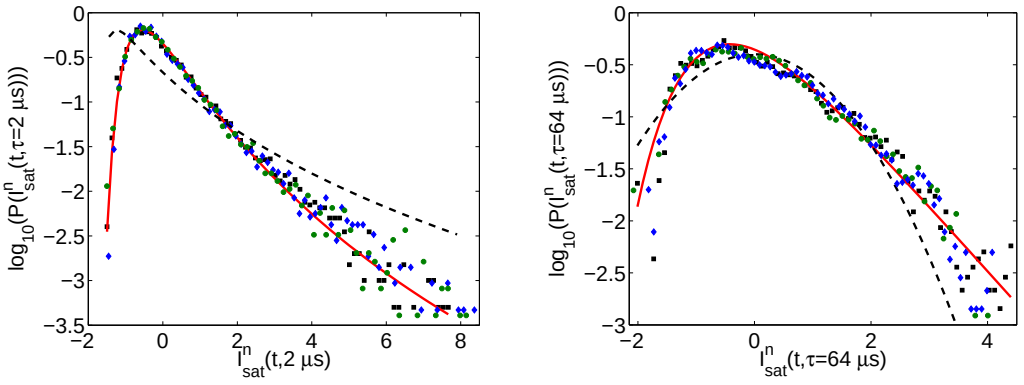

Figure 4: Measured frequency of occurrence of values of: (left) $\delta I_{sat}(t,\tau=2\mu s)\equiv I_{sat}(t)$, see Eq.(1); (right) $\delta I_{sat}(t,\tau=64\mu s)$. These semi-logarithmic plots are for all three MAST plasmas; black $\square-14218$, blue $\diamond-14219$, green $\circ-14220$. Solid lines represents the best visual fit of: (left) the Fréchet distribution with index $k=1.25$; (right) the Gumbel distribution with $a=1.4$. Dashed lines show: (left) a log-normal distribution and (right) a normal distribution whose mean and standard deviation are calculated from the data set of plasma 14220.

distributions respectively. The PDF of the fluctuations from all the MAST plasmas considered, sampled on a timescale $\tau=2\mu$s, is well fitted by an extremal, Fréchet distribution with index $k\approx 1.25$. The PDFs on temporal scales $\tau>40\mu$s, beyond the transition noted in Fig. 3, are shown in Fig 4(right) together with the Gaussian and the Gumbel distribution plotted over experimental data. The normal distribution does not capture negative fluctuations well and departs visibly from the measured PDF for fluctuations larger than 3σ. The Gumbel distribution with $a=1.4$ gives a satisfactory description of the entire PDF.

Conclusions. We have identified two regions of approximately self-similar scaling in structure functions of the δI_{sat} fluctuations. Similar values of scaling exponents α suggest universality of the edge plasma turbulence, independent of the edge magnetic field configuration when close to double null. These two different scaling regimes are separated by a transition region at $\tau\approx 40-60\mu$s. We find that extreme value Fréchet and Gumbel distributions model the rescaled PDFs P_s of the fluctuations, with remarkably good agreement in the two turbulence regimes.

Acknowledgements: This work was supported in part by the EPSRC and by Euratom.

References

[1] S. Zhu *et al.*, Plasma Sci. Technol. **8**, 118 (2006)
[2] H. Meyer *et al.*, Nucl. Fusion **46**, 64 (2006)
[3] G. Y. Antar, G. Counsell, Y. Yu, B. Labombard, P. Devynck, Phys. Plasmas **10**, 419 (2003)
[4] B. Ph. van Milligen *et al.*, Phys. Plasmas **12**, 052507 (2005)
[5] B. D. Dudson *et al.*, Plasma Phys. Control. Fusion **47**, 885 (2005)
[6] R. O. Dendy and S. C. Chapman, Plasma Phys. Control. Fusion **48**, B313 (2006)
[7] B. Lloyd *et al.*, Plasma Phys. Control. Fusion **46**, B477 (2004)
[8] A. Kirk *et al.*, Plasma Phys. Control. Fusion **48**, B433 (2006)